Bioresource Technology 348 (2022) 126788

Contents lists available at ScienceDirect

Bioresource Technology

journal homepage: www.elsevier.com/locate/biortech

Review

Cathodic biofilms – A prerequisite for microbial electrosynthesis

Igor Vassilev [a], Paolo Dessì [b], Sebastià Puig [c], Marika Kokko [a,*]

[a] Faculty of Engineering and Natural Sciences, Tampere University, Korkeakoulunkatu 8, 33720, Tampere, Finland
[b] School of Chemistry and Energy Research Centre, Ryan Institute, National University of Ireland Galway, University Road, H91 TK33 Galway, Ireland
[c] LEQUIA. Institute of Environment. University of Girona, Carrer Maria Aurèlia Capmany 69, 17003, Girona, Spain

HIGHLIGHTS

- Resilient and robust biofilms are required for microbial electrosynthesis.
- Biocompatible materials reinforce microbial adherence and growth.
- Substrate and nutrient availabilities could limit biofilm development.
- Counter reaction plays a role in the evolution of cathodic electro-active biofilms.
- Long-term studies are required to understand their effects on cathodic biofilms.

GRAPHICAL ABSTRACT

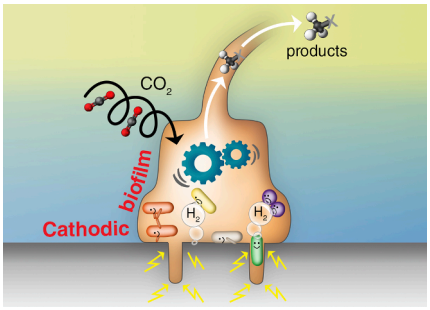

ARTICLE INFO

Keywords:
Biocatalyst
Bioelectrochemical system
Biocompatible materials
Carbon capture and utilization
Electroactive biofilm

ABSTRACT

Cathodic biofilms have an important role in CO_2 bio-reduction to carboxylic acids and biofuels in microbial electrosynthesis (MES) cells. However, robust and resilient electroactive biofilms for an efficient CO_2 conversion are difficult to achieve. In this review, the fundamentals of cathodic biofilm formation, including energy conservation, electron transfer and development of catalytic biofilms, are presented. In addition, strategies for improving cathodic biofilm formation, such as the selection of electrode and carrier materials, cell design and operational conditions, are described. The knowledge gaps are individuated, and possible solutions are proposed to achieve stable and productive biofilms in MES cathodes.

1. Introduction

Decarbonization of industry and circular economy are priorities worldwide, raising the attention towards carbon capture and utilisation technologies. Among them, microbial electrosynthesis (MES) is a potential bioelectrochemical process to convert CO_2 to a wide range of short-chain carboxylic acids, alcohols and methane, most of which are currently produced from fossil-based precursors (Dessì et al., 2021a; Prévoteau et al., 2020).

After more than ten years from its conceptualisation (Nevin et al., 2010), MES still suffers of some major challenges, including high capital costs and low production rates and titers that prevent its adoption in industry (Jourdin et al., 2020; Prévoteau et al., 2020). The low production rates, associated with the low current densities achieved so far, are arguably the main challenges towards MES maturity. To date, the highest current densities reported in MES cells are in the order of 100 A/m^2 (Jourdin et al., 2018), at least one order of magnitude lower than those reported in abiotic CO_2 electrolysers, resulting in carboxylic acid

* Corresponding author.
E-mail address: marika.kokko@tuni.fi (M. Kokko).

https://doi.org/10.1016/j.biortech.2022.126788
Received 26 November 2021; Received in revised form 24 January 2022; Accepted 25 January 2022
Available online 30 January 2022

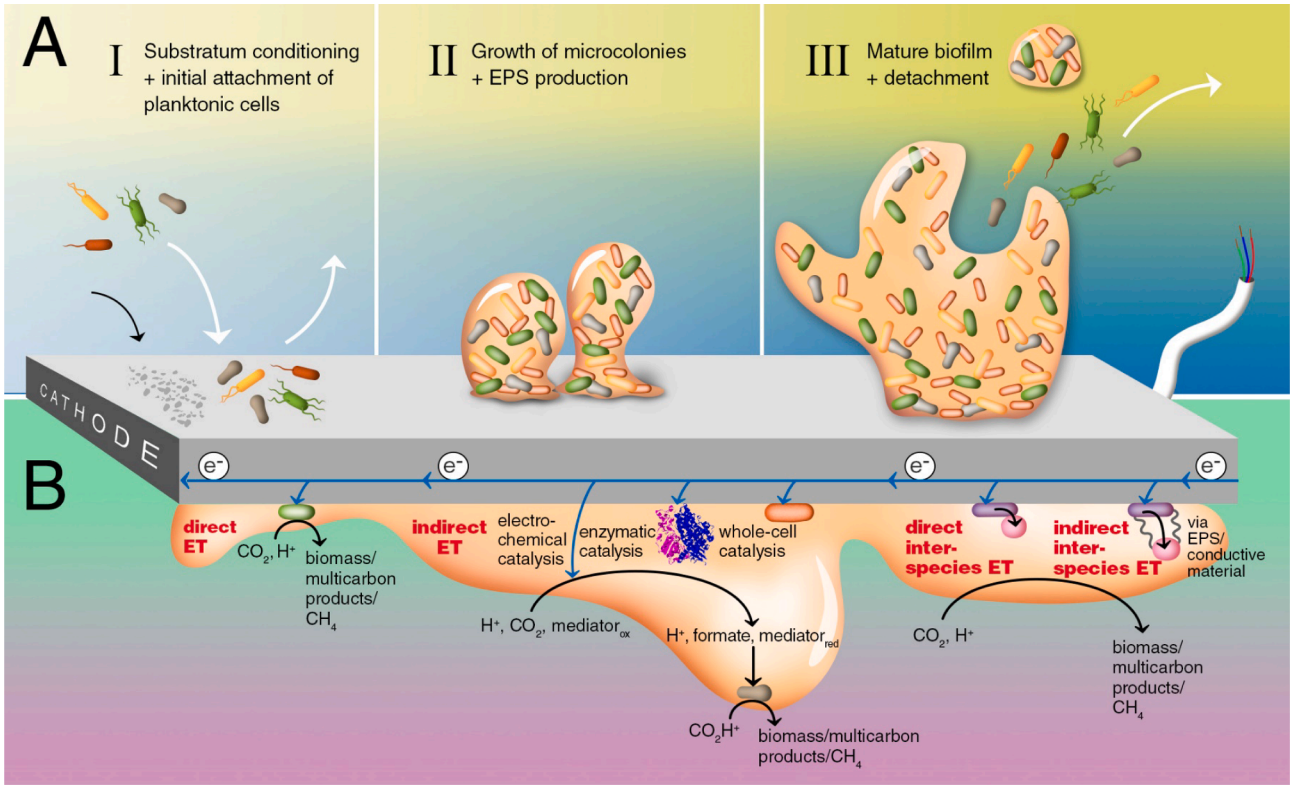

Fig. 1. Putative biofilm development and microbial electron uptake mechanisms on the cathode. (a) Simplified schematic representation of three-stage biofilm development from the single attachment of planktonic cells to mature biofilms. (b) Simplified illustration of direct and indirect electron transfer (ET) from the cathode and between species.

production rates below 1 kg/m^2/d (Prévoteau et al., 2020).

The production rates and efficiency of MES highly depend on the interaction between microorganisms and electrodes. Close microbe-cathode interaction enables a local uptake of the reducing equivalents required for CO_2 reduction (Kracke et al., 2015; Tremblay et al., 2017). This can mitigate mass transfer limitations in MES, and enable higher product yields than the well-established gas fermentation (Wood et al., 2021). So far, the highest current densities, coulombic efficiencies and production rates were indeed achieved in MES cells equipped with 3D structured cathode electrodes hosting well-structured, relatively thick (5–10 μm) electroactive biofilms (Jourdin et al., 2015). Higher current densities of about 500 A/m^2 can be theoretically achieved by very thick (100 μm), conductive and metabolically active biofilms (Claassens et al., 2019).

Thus, promoting the biofilm growth on MES cathodes is of utmost importance. These biofilms should be robust and resilient to withstand variable feed gas composition, flow rates, fluctuating cathode potential and current densities. This review aims to: (i) describe the fundamentals of cathodic biofilm formation in MES cells, (ii) give an overview of the research efforts conducted on promoting biofilm formation, and (iii) provide insight on strategies to develop productive and resistant biofilms for the application of MES in industry.

2. Cathodic biofilms

2.1. Biofilm development on a cathode

In nature, microorganisms predominantly live in biofilms, communities of sessile cells embedded in self-produced extracellular polymeric substances (EPS), which protects the microorganisms against harsh environments (Costerton et al., 1995). EPS consist mainly of polysaccharides, proteins, and lipids, and includes minor amounts of humic acids, uronic acids, and nucleic acids (Flemming and Wingender, 2010).

Biofilm development greatly depends on numerous factors such as microbial species, environmental conditions, hydrodynamics and properties of the surface to be colonized, i.e. the cathode in the case of MES. The heterogeneous biofilm formation undergoes very complex regulations, which can be simplified and described in three stages (Fig. 1A) (Berlanga and Guerrero, 2016). In the first stage, the cathode is conditioned by organic and inorganic macromolecules creating a nutritious settlement area for planktonic cells. In this stage, planktonic cells continuously attach to, and detach from, the cathode. Besides, some cells attach irreversibly and introduce the second stage of reproduction and EPS secretion on the cathode. EPS bind the cells to the cathode and each other, thereby supporting the development of stable and robust 3D biofilm structures (third stage). The mature biofilm embeds channels and pores to allow water, nutrients and products diffusion through the complex biofilm architecture. In the terminal process of biofilm life-cycle, some biofilm-dispersed cells detach due to shear forces and initiate new microcolony proliferation (Berlanga and Guerrero, 2016; Halan et al., 2012). A steady state biofilm thickness is reached when an equilibrium between biomass growth and detachment is achieved.

The described development of cathodic biofilms is based on the assumption that biofilms develop on cathodes in a comparable way as on other well-studied non-conductive surfaces. However, the different development stages of cathodic biofilms have been hardly studied in MES, and often limited to microscopy and 16S rRNA-based microbial community analysis on mature biofilms (Table 1).

In natural and engineered systems, heterotrophic microorganisms can form thick biofilms of several mm (Halan et al., 2014). However, thin autotrophic biofilms of few micrometres or even just single-cell layers are often developed in MES due to limited carbon or/and energy uptake (Izadi et al., 2020). Only recently researchers achieved cathodic biofilm growth of several hundreds micrometres thickness (Jourdin et al., 2018; Wang et al., 2020). An adequate amount of biofilm on the cathode as the biocatalyst is a prerequisite for high production

Table 1
Strategies applied for promoting biofilm formation in MES cathodes, and resulting biofilm characteristics and production rates.

Inoculum	Approach for promoting biofilm formation	Operation mode	pH	T (°C)	V_{cat} (V *vs.* SHE)	I (A/m^2)	Products (main product in bold)	Production rate (main product)		CE (%)	Biofilm characteristics	Reference
								g/m^2/d	g/L/d			
Isolated *Eubacterium limosum*	Tubular chamber filled with graphite granules to increase active surface	Batch	5.3–5.9	25	−0.8	0.3–0.6	**Acetate**, ethanol	0.081	*n.a.*	14	*n.a.*	(Blasco-Gómez et al., 2019)
Enriched, heat-treated mixed culture	Circular-shaped flow cell equipped with gas diffusion electrode (GDE) to increase availability of gaseous substrates on the electrode surface	Batch	5–6	30	−0.9	20	**Acetate,** butyrate, ethanol	36.6	0.06	35	Microbial biofilm and aggregates visible on the GDE surface (SEM)	(Bajracharya et al., 2016)
Enriched mixed culture	Glass vessel partially filled with graphite granules to increase active surface	Batch	5	35	−0.8	9 ± 3	**Acetate**, butyrate, isobutyrate, caproate, ethanol, butanol, hexanol	*n.a.*	0.14	*44*	Prevalence of *Clostridium* and detection of genes involved in acetogenesis, solventogenesis and chain elongation (Metagenomic analysis)	(Vassilev et al., 2018)
Enrichment culture	Polydopamine and Mo_2C on carbonized loofah sponge to increase specific area, electron and mass transfer, and accelerate hydrogen release	Batch	6.8	25	−0.85	0.15	**Acetate**	167	0.15	*68*	Thick biofilm (SEM) containing 265 μg/cm^2 of proteins dominated by *Acetobacterium* and *Arcobacter* (sequencing)	(Huang et al., 2021)
Enrichment culture	Fabrication of reduced graphene oxide/biofilm on carbon felt to improve electron exchange	Batch	7.0	25	*−0.85*	4.9	**Acetate**	*9.5*	0.17	*77*	Biofilm of 12 μm thickness (CSLM) dominated by *Acetobacterium* (sequencing)	(Song et al., 2017)
Engineered *Clostridium ljungdahlii*	Nickel phosphide deposition on carbon felt to decrease hydrogen evolution reaction (HER) overpotential	Batch	*n.a.*	25	−0.85	5.64	**Acetate/butyrate**, ethanol	*n.a.*	0.17/ 0.1	*82*	Pure culture of engineered *C. ljungdahlii* produced a 600 μm thick biofilm (LSCM) with more live cells than control	(Wang et al., 2020)
Enrichment culture	Glass vessel with Mo_2S nanoflowers on carbon felt to improve electron transfer	Batch	*n.a.*	25	−0.85	0.06	**Acetate**	*n.a.*	0.2	*58*	Bacteria adhered to the porous nanoflower structure (SEM), high abundance of *Arcobacter* and *Acetobacterium* (sequencing)	(Song et al., 2020a)
Enrichment culture	Prussian blue nanocube -modified carbon felt to enhance hydrophilicity and create a positive surface charge	Batch	6.8	25	−0.85	4.5	**Acetate**	*n.a.*	0.20	*63*	Dense biofilm of 50 μm thickness (FESEM + CLSM), dominated by *Arcobacter* and *Acetobacterium* (sequencing)	(Tian et al., 2020b)
Enrichment culture	Perovskite amended carbon felt to increase hydrophilicity, CO_2 adsorption and H_2 production	Batch	6.8	25	−0.85	0.56	**Acetate**, formate, ethanol, butyrate	*n.a.*	0.2–0.24	*73*	Dense biofilm of 430 μm thickness (LSCM + SEM) with about 260 μg/cm^2 protein content, dominated by *Acetobacterium*, *Arcobacter*, and *Sulfurospirillum* (sequencing)	(Tian et al., 2020a)
Enriched mixed culture	Activated carbon slurry (20 μm average particle size) to maximize mass and charge transfer	Batch	7–7.5	30	*n.a.*	14 mA[b]	**Acetate**, methane, isobutyrate, propionate	*n.a.*	0.72[c]	*n.a.*	*n.a.*	(Jiang et al., 2020)
Activated sludge	Carbon paper coated with redox mediators neutral red (NR) and methyl viologel (MV) incorporated with PANI to improve electron exchange	Fed-batch	6.8	*n.a.*	*−0.85*	14.8	**Acetate**, ethanol	*197*	n.a.	*55*	Porous biofilm obtained with MV, denser biofilm with NR which limited diffusion (SEM)	(Anwer et al., 2021)
Stormwater pond sediment and wastewater treatment plant	Glass vessel with NanoWeb-RVC deposited by CVD[d] (above) or EPD[e] (below) to maximise surface:volume ratio, mass-transfer and conductivity	Fed-batch	7	35	*−0.85*	37 102	**Acetate**	192 685	*n.a.*	*70* *100*	High density of 1–2 μm rod-shaped cells, more EPS visible in the CVD than in the EPD electrode (SEM); copper detected in the electrode by EDS	(Flexer and Jourdin, 2020)
Enrichment culture	Copper ferrite /reduced graphene oxide composites on carbon cloth to	Fed-batch	6.8–8.1	35	−0.54	2.92	**Isobutyrate/ acetate**	31.0/ 4.3	*n.a.*	*77*	Dense biofilm (in comparison to control) (FESEM[f]) with prevalence of	

(*continued on next page*)

Table 1 (*continued*)

Inoculum	Approach for promoting biofilm formation	Operation mode	pH	T (°C)	V_{cat} (V *vs.* SHE)	I (A/m^2)	Products (main product in bold)	Production rate (main product)		CE (%)	Biofilm characteristics	Reference
								g/m^2/d	g/L/d			
	increase surface area and decrease HER overpotential										*Betaproteobacteria*, *Bacteroidetes* and *Firmicutes* (sequencing)	(Thatikayala and Min, 2021)
Enriched mixed culture	Chamber containing granular activated carbon (GAC) fluidised by magnetic stirring to increase contact between microorganisms and substrates	Continuous	*n.a.*	25	−0.85	4.1	**Acetate**	15.7	0.14	65	GAC increased cell attachment on carbon felt collector (SEM); prevalence of *Proteobacteria* and *Firmicutes* on carbon felt and GAC (sequencing)	(Dong et al., 2018)
Anaerobic sludge	TiO_2 or Rh on carbon felt to decrease the HER overpotential and avoid electrostatic repulsion	Continuous	7.0	27	*−0.9*	7.26	**Acetate**, propionate, butyrate	*268*	2.15	*73*	Scattered cells on the electrode, with higher colonization in the TiO_2 coated electrode (SEM)	(Das et al., 2021)
Enriched mixed culture	Flow-through chamber with three layers carbon felt electrode and nutrients supplementation to develop a thick biofilm on the whole felt thickness (1.2 cm deep)	Continuous	5.8	32	−0.85	80–100	**Acetate**, butyrate, caproate	*n.a.*	9.8	88	Thick and uniform biofilm on carbon felts, including interspaces, with microorganisms of various morphologies (rods of 1–10 μm and filaments up to 300–400 μm) (SEM)	(Jourdin et al., 2018)
Isolated *Eubacterium limosum*	Tubular chamber filled with graphite granules to increase active surface	Batch	5.6–6.1	25	−0.8	0.3–0.6	**Ethanol**, acetate	0.158	0.13	12	*n.a.*	(Romans-Casas et al., 2021)
Enrichment culture	Graphene oxide and PEDOT[g] modified carbon cloth to promote electron transfer, specific area and avoid electrostatic repulsion	Batch	*n.a.*	*n.a.*	−0.7	2.54	**Methane**	5.1	n.a.	*89*	Around 18.7 mg biofilm with rod-like microorganisms and EPS (SEM), denser than the control, dominated by *Methanobacterium* (sequencing)	(Li et al., 2020a)
Anaerobic granular sludge	Chamber containing a granular sludge bed to increase biomass density and resilience, and avoid washout	Batch	7–7.5	37	−1.84[a]	68	**Methane**	133	0.43	85	Granular sludge community dominated by *Methanobacterium* (sequencing)	(Zhou et al., 2021)

[a] Applied cell voltage of 5.5 V; [b] Galvanostatic control, electrode surface not reported; [c] Not reported, estimated from the graph; [d] Chemical vapor deposition; [e] Electrophoretic deposition; [f] Field emission scanning electron microscopy; [g] poly-(3, 4-ethylenedioxythiophene).

rates in MES. However, excessive growth of biomass on the cathode might result in mass transfer limitations in the thick biofilm. In microbial fuel cells, thick anodic biofilms (100–200 μm) can suffer from electron- and mass-transport limitations, which may result in an increased amount of inactive bacteria in the biofilm leading to poor current generation (Babauta and Beyenal, 2014; Sun et al., 2016, Sun et al., 2015). Therefore, the thickness of cathodic biofilms should not limit the availability of nutrients, CO_2 and reducing equivalents within the biofilm but should allow growing a sufficient amount of metabolic active cells for high CO_2 turnover.

2.2. Uptake of reducing power by cathodic biofilms

Biofilm growth and MES productivity greatly depend on the microbial capability of uptaking reducing equivalents from the cathode. However, the knowledge on electron transfer from a cathode to autotrophic cells is limited (Karthikeyan et al., 2019; Tremblay et al., 2017). The putative direct and indirect electron transfer (ET) mechanisms are described in Fig. 1B. Direct ET relies on physical cell-cathode contact (Cheng et al., 2009). Direct ET mechanisms were mainly studied in anodic applications, where microorganisms transfer electrons to anodes using them as electron sinks. Such processes typically involve outer-membrane-bound cytochromes facilitating the ET from the cell interior across the membrane to the anode (Xu et al., 2021). It was also proposed that cytochromes play a role in direct electron uptake from the cathode. However, while some of the autotrophs possess outer-membrane-bound cytochromes (e.g., *Moorella, Sporomusa* and *Methanosarcina*) others do not (e.g., *Clostridium*) while still showing capabilities of direct ET (Faraghiparapari and Zengler, 2017; Nevin et al., 2011; Rowe et al., 2019; Yu et al., 2017). Some pure cultures of the genus *Clostridium, Moorella, Sporomusa* and *Methanosarcina* showed current consumption for CO_2 reduction at −0.4 V and/or −0.3 V *vs*. standard hydrogen electrode (SHE), supporting the hypotheses of direct electron uptake (Faraghiparapari and Zengler, 2017; Nevin et al., 2011; Rowe et al., 2019; Yu et al., 2017).

Direct ET occurs not only between electrode and microorganisms but also between different microorganisms. Direct interspecies ET builds upon physical cell–cell contact, where one species transfers electrons to another. Such syntrophic ET strategy was mainly studied with methanogens, in particular, coupling *Geobacter* with *Methanosarcinales* (Rotaru et al., 2014). In this co-occurrence, *Geobacter* performs ET via electrically conductive appendages. However, the mechanism of how *Methanosarcinales* takes up electrons is uncertain (Yee and Rotaru, 2020).

Indirect ET involves the production of a mediator at the cathode, which functions as an electron carrier for the autotrophs. At cathodic potentials below −0.4 V *vs*. SHE, H_2 evolution reaction (HER) can occur via water hydrolysis, and the produced H_2 can then be utilized by acetogens or methanogens (Blanchet et al., 2015). However, depending on pH and H_2 partial pressure, the threshold for HER can vary. Besides, it was hypothesised that some hydrogenotrophic microorganisms maintain low H_2 partial pressures at the cathode as a strategy to enhance HER, which makes it challenging to determine whether MES is facilitated by direct or H_2 mediated ET even at cathodic potentials higher than −0.4 V *vs*. SHE (Philips, 2020). On the other hand, with *Acetobacterium* sp. current consumption was only observed at a negative potential of −0.71 V *vs*. SHE, clearly indicating that the electron uptake was mediated by electrochemically produced H_2 (Arends, 2013; Nevin et al., 2011). Similarly, in MES inoculated with mixed cultures, acetogens or methanogens were cultivated at cathodic potentials below −0.5 V *vs*. SHE, likely promoting mediated ET mechanisms (Table 1).

Formate is another intermediate that can be electrochemically produced at negative cathodic potentials on electrode materials such as indium (Gimkiewicz et al., 2017). Besides abiotic production, H_2 and formate can also be biotically synthesized by cell-free enzymes and whole cells attached to the cathode. For example, Deutzmann et al. (2015) discovered cell-free cathode-associated hydrogenases and presumably formate dehydrogenases, which were likely secreted by living cells or originated from lysed dead cells. It was proposed that the enzymatically produced hydrogen and formate supported *Methanococcus maripaludis* in the supply of reducing power for the conversion of CO_2 into methane (Deutzmann et al., 2015). Perona-Vico et al. (2020) indicated several bacteria of the genus *Rhodobacter*, *Rhodocyclus*, and *Desulfovibrio* as potential H_2 producers for microbial electrosynthesis. *Desulfovibrio paquesii* and *Desulfovibrio desulfuricans* were the most efficient, achieving eight-fold higher production rates than the abiotic control at an applied potential of −0.8 V *vs*. SHE. Based on metabolic reconstruction and modelling of a mixed MES community, another study hypothesized that H_2 and formate were produced by *Desulfovibrio* cells. Subsequently, H_2 and formate were consumed by *Acetobacterium* for acetate production from CO_2 (Marshall et al., 2017). Such a syntrophic microbial interaction can also be seen as indirect interspecies ET. Besides H_2 and formate, indirect ET can also be facilitated between different species via EPS. EPS comprise electrochemical active substances (*e.g.*, flavins and c-type cytochromes), which support long-distance ET putatively by electron hopping mechanisms (Yong et al., 2022). Further, microorganisms can attach to suspended conductive material in the medium such as magnetite or granular activated carbon and exchange electrons via reduction/oxidation of the material (Lovley, 2017).

Another example of indirect electron transfer is the supply of microorganism with artificial redox active compounds (mediators), which can shuttle electrons between electrode and microorganisms. Methyl viologen was shown to facilitate ET from the cathode to *Moorella thermoacetica and Clostridium formicoaceticum* enabling the conversion of CO_2 into formate (Song et al., 2011). In anodic applications, it was demonstrated that mediators such as flavins and phenazines can be produced naturally by *Shewanella oneidensis* and *Pseudomonas aeruginosa*, respectively, but in cathodic applications, mediator excretion by autotrophs has not been reported so far (Martinez and Alvarez, 2018).

2.3. Energy conservation in cathodic biofilms

The growth of chemoautotrophic biofilms in MES is very slow due to the limited cellular energy generated using CO_2 and the electrode as the sole carbon and energy source, respectively. Based on a thermodynamic model, the growth rate of an acetogenic cathodic biofilm was calculated as 0.12 d^{-1}, which is 1 to 2 magnitude lower than for heterotrophs such as *Escherichia coli* (Cabau-Peinado et al., 2021; Gibson et al., 2018). Acetogens and methanogens gain only 0.3 to 1 mol ATP per mol acetate or methane produced, respectively, when ET is mediated through H_2 or formate (Katsyv and Müller, 2020; Thauer et al., 2008). CO_2 is metabolised via the reductive acetyl-coenzyme A pathway, also known as the Wood-Ljungdahl pathway. However, on the substrate-level phosphorylation, no net ATP is yielded. Instead, CO_2 reduction and H_2 oxidation are coupled with an electron-transport phosphorylation module making it possible to gain ATP and live at the thermodynamic edge of life (Katsyv and Müller, 2020; Thauer et al., 2008). In detail, an electron-bifurcating hydrogenase enzyme supports cellular energy saving by splitting the electron transfer flow from H_2 to an exergonic and endergonic reaction reducing NAD^+ and ferredoxin, respectively (Buckel and Thauer, 2018). In the next step, membrane-bound respiratory enzymes, Rnf (energy-converting ferredoxin: NAD^+ reductase complex) or Ech (energy-converting ferredoxin-dependent hydrogenase complex) use the reduced ferredoxin to reduce NAD^+ or protons. Rnf and Ech exploit the free energy change of the electron transport to generate an electrochemical ion gradient (H^+ or Na^+) across the membrane and thereby drive the ATP synthesis via ATPase (Katsyv and Müller, 2020; Thauer et al., 2008). The Wood-Ljungdahl pathway and the coupled electron-transport phosphorylation pathway vary in enzymes and reactions among acetogens and methanogens and different species within those groups resulting in different net ATP yields (Sousa and Martin, 2014). For example, it was observed that methanogens possessing cytochromes

generate higher cellular energy than methanogens without cytochromes (Mand and Metcalf, 2019). For a comprehensive review on energy conservation mechanisms of acetogens and methanogens, the reader is referred to Katsyv and Müller (2020) and Thauer et al. (2008). Whether the energy conservation mechanism via utilisation of H_2 or formate is similar to the mechanism when electrons are taken up directly from the cathode is uncertain, as the direct ET mechanisms are not known yet.

2.4. Characterization of cathodic biofilms

Surface morphologies of biofilms have been mostly characterised with scanning electron microscopy (SEM) after biofilm fixation, while the biofilms were phylogenetically characterised with sequencing (Table 1). In addition, biofilm imaging has been done with confocal laser scanning microscopy (LSCM) combined with biofilm thickness measurements and/or staining with live/dead (Wang et al., 2020) or hydrogenotrophic/acetoclastic methanogen-specific probes (Yang et al., 2020). The biomass content in the biofilm has been estimated by measuring the protein content (Huang et al., 2020; Xiang et al., 2017). EPS have been separated from the cells by sonication and their composition have been analysed via three-dimensional excitation-emission matrix fluorescence spectroscopy or colorimetric methods such as the phenol-sulfuric acid method and Bradford assay to determine exopolysaccharide and exoprotein concentrations, respectively (Hou and Huang, 2020; Qian et al., 2019). These methods, however, are invasive and often require dismantling the MES cells. Online biofilm characterisation or monitoring has been rarely done on cathode electrodes resulting in a limited knowledge on biofilm development over time. Hackbarth et al. (2020) monitored the growth of *Kyrpidia spormannii* biofilm, producing storage polymer polyhydroxybutyrate, in a flow cell by 3D optical coherence tomography that enabled monitoring biofilm growth over time along the length of the cathode. The development of further live in-vivo characterisation methods is crucial to understand the biofilm development from single cells to mature communities of sessile cells, which will allow to improve the start-up of MES reactors and the growth of thick biofilms.

3. Strategies to promote biofilm formation in MES cells

The following sections explore in detail cathode materials and innovative cell designs proposed in MES to promote the development of electrotrophic biofilms over the planktonic microbial communities. Some of these strategies and their effects on biofilm characteristics have also been gathered in Table 1.

3.1. Cathode materials

Increasing the electrode surface area (Flexer and Jourdin, 2020), creating positive surface charge (Das et al., 2021), enhancing hydrophilicity (Tian et al., 2020a), and conductivity (Thatikayala and Min, 2021) have proven effective in increasing biofilm formation in MES cathodes. In MES, carbon is often used as the electrode material due to its biocompatibility, chemical stability, and low cost. Since often used carbon materials, such as felts, clothes or plates, have low surface areas, 3D-structured carbon materials were proposed to increase the surface available for biofilm formation. Flexer and Jourdin (2020) deposited carbon nanotubes on 3D-structured reticulated vitreous carbon (RVC) electrodes. The extremely high surface area obtained enabled the formation of a thicker biofilm compared to the bare RVC (see supplementary material), resulting in current densities above 100 A/m^2 and a record (so far) acetate production rate of 1330 g/m^2/d.

Metal addition can increase the conductivity of the electrode, create a positive surface charge, and a higher surface area for biofilm attachment. Nie et al. (2013) embedded anchored nickel nanowires on graphite to facilitate biofilm formation by a pure culture of *Sporomusa ovata* (see supplementary material). In another study (Das et al., 2021), coating carbon cloth with titanium oxide (TiO_2) resulted in lower charge transfer resistance, higher conductivity and positive surface charge. This promoted biofilm growth from a mixed culture in comparison to bare carbon cloth. Modification of carbon felt with nickel-phosphide also resulted in a thicker biofilm formation by engineered *Clostridium ljungdahlii* than bare carbon felt (see supplementary material), with 1.7- and 2.5-times higher acetate and butyrate production rates, respectively (Wang et al., 2020). However, the authors found that the biofilm formation was dependent on the number of electrodeposition cycles on Ni-P catalyst, and biofilm formation was inhibited after 20 cycles due to agglomeration of the catalyst (Wang et al., 2020).

Co-deposition of molybdenum carbide (Mo_2C) as well as polydopamine on carbonized loofah sponge with a 3-D macroporous structure resulted in thick biofilms (see supplementary material) (Huang et al., 2021). Similarly, growing Mo_2C *in situ* on carbon felt (Huang et al., 2020) or hydrothermal synthesis of Mo_2S on carbon fiber at 180 °C generated porous nanoflower structures (Song et al., 2020a) that enhanced biofilm formation and protein content (linked to biomass growth), improving H_2 production rates. Electrode modifications have also shown to affect the composition of the microbial communities in cathodic biofilms. For example, carbon felt with nickel ferrite promoted the development of *Proteobacteria* and *Thermotogae* (putative butyrate producers) and steered production towards butyrate (Tahir et al., 2021).

Electrode modifications with mediators, such as coating carbon paper with neutral red or methyl viologen, can enhance electron transfer (due to a lower charge transfer resistance). Methyl viologen resulted in a more porous biofilm (see supplementary material), and higher acetate production rates, than neutral red (Anwer et al., 2021). Similarly, high abundances of hydrogenotrophic and acetoclastic methanogens (observed with CLSM), and high methane production rates, were obtained by modifying carbon felt electrodes with neutral red or anthraquinone-2,6-disulfonate (AQDS) (Yang et al., 2020). Modification of carbon felt with Prussian blue nanocubes generated a hydrophilic cathode electrode with positive charge, with efficient electron transfer through Fe^{2+} and Fe^{3+} that hosted a two-fold thicker biofilm than bare carbon felt (Tian et al., 2020b). Self-assembled graphene oxide/biofilms have been successfully constructed to promote electron transfer between electrode and biofilm, and within the biofilm, achieving higher acetate production rates than pure carbon felt (Song et al., 2017).

Carbon cloth coated with the conductive polymer poly-(3,4-ethylenedioxythiophene) (PEDOT) and graphene oxide were characterized by high surface area and conductivity, promoting methanogenic biofilm formation (observed by SEM and biomass quantification), with methane production rates up to 5.1 g/m^2/d (Li et al., 2020a). Modifying gas diffusion electrodes with polyaniline (PANI) promoted HER and the growth of a butyrate producing biofilm (see supplementary material) compared to the control, although the biofilm thickness was similar (Fontmorin et al., 2021).

The addition of magnetite (Fe_3O_4) (Viggi et al., 2020), the application of a magnetic field (Song et al., 2020b) or a combination of both (Hou et al., 2021) have been reported to enhance acetate production from CO_2 in MES. The magnetic fields resulted in lower charge transfer resistance and enhanced biofilm growth (by 1.2 times, measured by protein content) by a pure culture of *Serratia marcescens* Q1, where the magnetic field enhanced the release of EPS (Song et al., 2020b). Besides stimulating EPS production by *S. marcescens* Q1, combined use of magnetic field and Fe_3O_4 resulted in an increased abundance of outer membrane c-type cytochromes (Song et al., 2020b). In addition, the magnetic field decreased leaching of iron from Fe_3O_4 compared to the sole use of magnetite (Hou et al., 2021).

3.2. Cell design

To date, the large majority of MES experiments have been conducted in conventional H-type cells operated in batch mode under mechanical stirring conditions (mainly magnetic stirring) (Dessì et al., 2021b;

Mohanakrishna et al., 2020). Such a configuration, besides being hardly scalable, suffers of low electrode surface for biofilm attachment, in particular when flat electrodes such as graphite plates or felts are used, and does not provide favourable hydrodynamic conditions for biofilm formation. Hence, innovative cell configurations are being explored to overcome these challenges.

A simple yet effective approach for increasing the surface area for biofilm adhesion in MES cells is to fill the cathode chamber with porous conductive materials, such as graphite granules, in contact with a current collector. Vassilev et al. (2018) operated a glass vessel cell with graphite granules as conductive carrier material for biofilm adhesion, reporting the production of carboxylic acids and alcohols up-to six carbon atoms chain. However, the detection of H_2 in the cell headspace suggests that the enriched microbial community, dominated by *Clostridium* sp., was mainly performing H_2-mediated electrosynthesis. Graphite granules were shown to host methanogenic biofilms in two-chamber MES (see supplementary material) (Batlle-Vilanova et al., 2015), and have been also proposed as carrier material in more scalable tubular MES cells. Blasco-Gómez et al. (2019) and Romans-Casas et al. (2021) reported concomitant acetic acid and ethanol production from CO_2 in tubular cells, although the low current density achieved (below 1 A/m^2) negatively impacted the production rates in such cell design.

Due to its capacitive nature, granular carbon material can be used in fluidised bed systems, where the biofilm-coated granules can cyclically re-charge by direct contact with a polarised collector, significantly improving mass transfer between microorganisms and electrolyte. Furthermore, carbon particles can stimulate interspecies electron transfer (Chen et al., 2014). Dong et al. (2018) reported an acetate production rate of 0.14 g/L/d from CO_2 in a H-type MES cell with a fluidised bed of granular activated carbon (GAC), 2.8 times higher than the control cell without GAC. To further increase the specific surface, activated carbon (AC) can be supplied as a powder to form a so-called "slurry electrode" (Jiang et al., 2020). Jiang et al. (2020) added 5 g/L AC with an average particle size of 20 μm, reporting a 179% increase of the acetate titre compared to a control cell without AC. Biologically produced granules can also enhance production rates in MES cells. Such an approach was proposed by Zhou et al. (2021), who fed a MES cell with anaerobic granular sludge to produce methane from CO_2 and electrochemically produced H_2 obtaining, to date, the highest production rate of 202 $L/m^2/d$.

Besides the active surface area of the cathode, the limited CO_2 solubilisation in aqueous media remains a main limitation in MES. Three-chamber cells equipped with a gas diffusion electrode (GDE) have been proposed to mitigate this issue (Bajracharya et al., 2016). GDEs combine a conductive catalytic layer (carbon-based for MES applications) to a polymeric, hydrophobic layer, resulting in a three-phase interphase that increases the CO_2 bioavailability on the electrode surface. This, in turn, promotes biofilm development on the electrode surface, mitigating the limitations of CO_2 solubilisation. Bajracharya et al. (2016) reported a full biofilm coverage of a GDE after 240-days cell operation, based on scanning electron microscope (SEM) imaging (although the biofilm thickness was not investigated), which resulted in an average production rate of 36.6 $g/m^2/d$ acetic acid from CO_2. The GDE-based reactor was shown also to support high-rate solventogenesis from CO_2 by mixed cultures, triggered by low pH (<5) and high acetate concentrations (>3 g/L), achieving, so far, the highest alcohol titre of 21 g/L (Srikanth et al., 2018).

Another strategy to improve the contact between the biocatalyst, electrolyte and inorganic carbon source, is the use of a flow-through system where the catholyte is forced to pass through the biofilm-covered electrode. This approach was adopted by Jourdin et al. (2018), who developed a cell design in which the catholyte was continuously recirculated through three layers of carbon felt (total thickness of 1.2 cm). This promoted the formation of a thick and morphologically heterogeneous biofilm (see supplementary material) on the whole electrode surface which enabled current densities as high as

Table 2
Effects of operation parameters on biofilm growth as well as on MES performance (all the cathode potentials are expressed against SHE).

Operation parameter	Effects on biofilm	Other effects	Reference
Cathode potential	Decreasing cathode potential from −0.51 to −0.61 V enhanced biofilm formation on the biocathode (SEM), while a further increase up to −0.91 V negatively affected biofilm density Biocathode potentials of −0.81 and −0.91 V accelerated H_2 generation hindering biofilm formation	Methane production rate increased up to 1.2 $g/m^2/d$ at −0.81 V Biocathodes started-up at −0.51 and −0.61 V produced methane also after increasing the potential to −0.31 V	(Li et al., 2020b)
	More efficient and conductive biofilm was formed at −0.49 V than at −0.36 and −0.53 V	The highest acetic acid yield of 35 mM was obtained at −0.49 V	(Ameen et al., 2020)
Cathode potential and inorganic carbon source	Highest biofilm coverage, thickness and proportion of live cells (CSLM, SEM) obtained at −0.81 V, while at −0.61 V no biofilm was observed Higher biofilm coverage, thickness and proportion of live cells obtained with CO_2 compared to $NaHCO_3$	CO_2 supply and −0.81 V applied potential resulted in the lowest HER overpotential, decreased charge transfer resistance (indicating highly conductive biofilm) and resulted in the highest production yield of organics, especially acetate	(Izadi et al., 2020)
Cathode potential and sulfate addition	Biofilm biomass content (measured as protein) and number of active cells (CSLM combined with live/dead staining) increased at decreasing cathode potentials from −0.31 to −0.61 V Addition of sulphate further increased biomass and active cells in the biofilm	Increased biofilm density resulted in enhanced acetate production and average current output up to 34.8 mM and 6.66 mA, respectively	(Xiang et al., 2017)
Oxygen diffusion to the cathode	The cathode was colonised by the adapted, oxygen-tolerant strain more efficiently than by the wild type (SEM)	Adaptive laboratory evolution of S. ovata was used to enhance the O_2 tolerance to 0.5–5% O_2 The adapted strain produced acetate 1.5-fold faster than the wild type	(Shi et al., 2021)
Temperature	Denser biofilms at 25 and 35 °C than at 55 and 70 °C, while at 10 °C only few scattered microbes (SEM, CSLM)	The highest acetate concentration (0.53 g/L) and production rate (0.049 g/L/d) obtained at 25 and 35 °C, respectively	(Yang et al., 2021)
Hydrodynamics	High flow velocities near the		(Hackbarth et al., 2020)

(*continued on next page*)

Table 2 (*continued*)

Operation parameter	Effects on biofilm	Other effects	Reference
	inlet resulted in denser and thinner biofilm of *Kyrpidia spormannii* (producing PHB) due to increased shear stress, while thicker biofilms were obtained towards the outlet with decreasing flow velocity (OCT)		

CLSM: Confocal laser scanning microscope, HER: hydrogen evolution reaction, OCT: Optical coherence tomography; PHB: polyhydroxybutyrate, SEM: scanning electron microscope.

175 A/m^2 with the consequent high-rate acetate production up to 9.8 g/L/d. In a subsequent study, the flow-through cell operation was optimised to promote chain elongation reactions by setting a high CO_2 loading rate (173 L/d) and hydraulic retention time (14 d), achieving the remarkable production rates of 3.3 and 2.0 g/L/d for butyrate and caproate, respectively. A similar approach was taken by Alqahtani et al. (2018) who utilised porous nickel hollow fibers to produce a three-phase interface for biofilm growth (see supplementary material), which included inorganic electrocatalyst for H_2 evolution, and a gas-transfer membrane for direct CO_2 delivery through the pores of the hollow fibers.

3.3. Operation parameters

The effects of operation parameters such as cathode potential, pH, inorganic carbon source, nutrients availability, H_2 partial pressure, and temperature on MES efficiency are widely studied (Blasco-Gómez et al., 2019; Das et al., 2020; Rovira-Alsina et al., 2021; Xiao et al., 2020), but detailed investigations of their effects on biofilm formation, growth and characteristics are scarce (Table 2). In addition, the results are not directly comparable as the biofilm growth and MES performance are

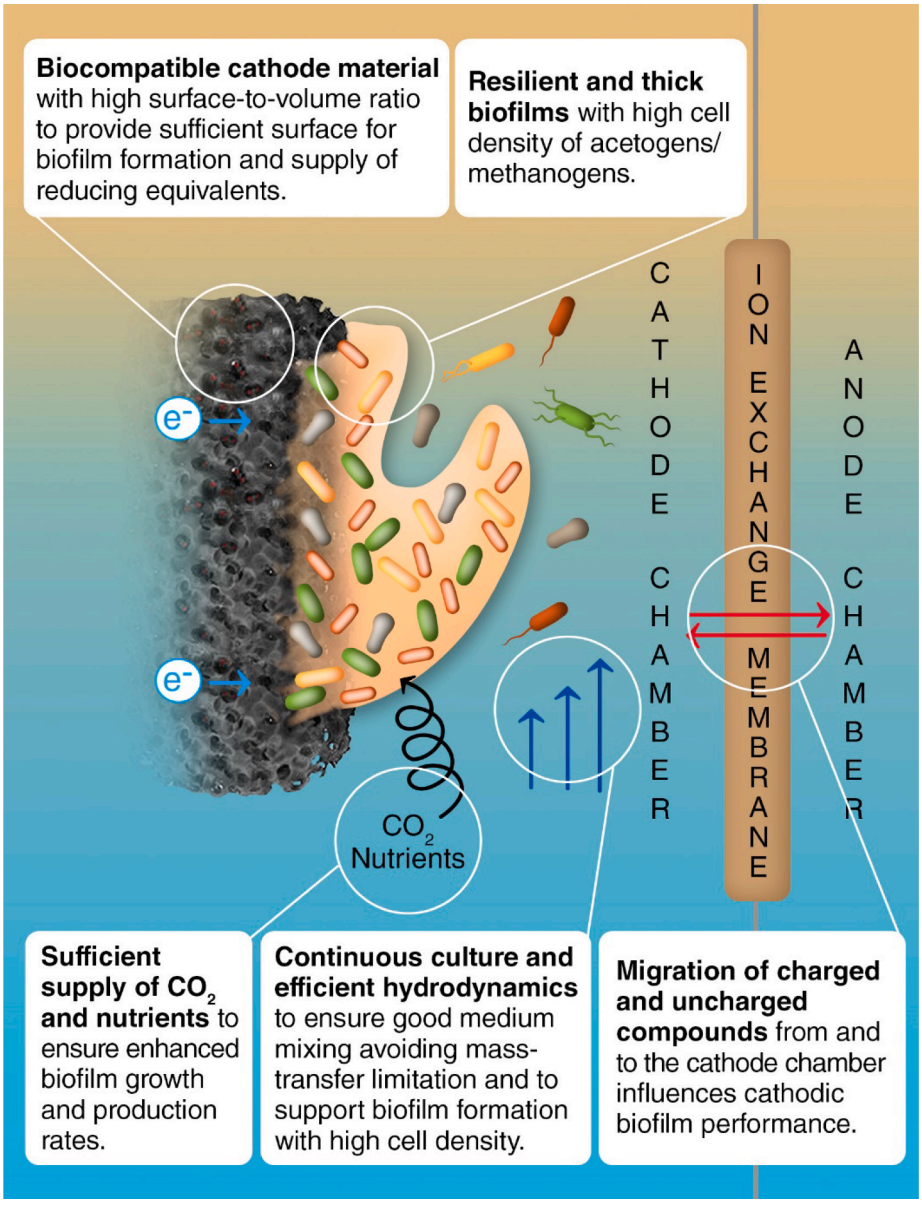

Fig. 2. Operation factors affecting biofilm development on MES cathodes.

affected by multiple parameters, *e.g.*, by the inoculum source, experiment time, electrode configuration and material, products of interest, and hydrodynamics. The optimal cathode potential for biofilm formation depends on experimental set-up and while higher biomass usually results in higher production rates and/or yields (Table 2), this is not always the case (Li et al., 2020b). Xiang et al. (2017) operated MES cells at cathode potentials ranging from −0.5 to −0.8 V, with and without the addition of sulfate, and investigated the thickness and viability of the resulting biofilms by CLSM combined with life/dead staining. Results showed that, regardless of the biofilm thickness obtained (from 23.75 to 43.38 μm), the highest portion of live cells was in the middle of the biofilm, while accumulation of dead cells was observed in the top and inner layer of the biofilm.

Poor information is available on the effect of inorganic carbon source, oxygen diffusion, temperature and hydrodynamics on biofilm generation (Table 2). Modelling of acetogenic MES revealed that a higher biofilm density can be achieved under continuous rather than batch operation, likely due to a constant replenishment of nutrients, product removal and washing out of planktonic cells (Cabau-Peinado et al., 2021). Similar observation was experimentally validated by Jourdin et al. (2018), who obtained thick biofilms with a continuous nutrient supply.

4. Outlook

The roadmap for the market application of MES is linked to the development of resilient and robust biofilms for long-term operation. Biofilms should adapt to the dynamic conditions of MES operation (i.e., intermittent and variable CO_2 feeding, pH gradients, intermittent power supply, and different pH_2). This is not straightforward, and several actors could play a role (Fig. 2). For instance, the counter-reaction at the anode (mostly water oxidation to oxygen and protons) influences the microbial community present in the electroactive cathodic biofilm. Batlle-Vilanova et al. (2015) found that *Methylocystis* sp. can oxidise methane using the oxygen diffused from the anode as electron acceptor. Lai et al. (2017) proposed a graphite electrode as a "sacrificial anode" to limit oxygen production and avoid its diffusion towards the cathodic biofilm. This is an interesting approach, but further investigation is needed to avoid the high capital costs of the anode electrodes (Jourdin et al., 2020).

Recently, a next generation of electroactive cathodic biofilms is popping up thanks to the application of 3D printing and modelling tools. Krige et al. (2021) developed a 3D-printed synthetic biofilm with embedded *S. ovata* cells for MES. Results indicated a significant decrease of the start-up time (about 40 h) and an acetate production rate of 104 g/m^2/d (0.68 g/L/d), one order of magnitude higher than typical *S. ovata* production rates in H-type cells, and 2–3 fold higher than reactors using specialized cathodes. Novel 3D-printed cathodes, consisting of carbon aerogel coated with NiMo-alloy to promote H_2 evolution, were proposed for electromethanogenesis (Kracke et al. 2021). Results showed a remarkable volumetric methane production rate of 2.2 $L/L_{catholyte}$/day (99% of coulombic efficiency) by *Methanococcus maripaludis*. Such promising results need to be complemented with long-term studies.

The first simulation studies in MES indicated that continuous CO_2 feeding allows the formation of dense biofilms and to achieve higher current densities (Cabau-Peinado et al., 2021). Further studies should be conducted to confirm such a hypothesis, and MES modelling should be amended to predict substrate diffusion, biomass attachment-decay and transfer or reducing equivalents within the biofilm.

Finally, the synergistic approach of using microalgae-bacteria biofilms is gaining the attention of the research community. These symbiotic relationships improve algal biomass production and enrich the biomass with valuable chemical and energy compounds. New studies on the topic are popping up with promising results in wastewater treatment. In the specific case of cathodic biofilms in MES, the relationship between microalgae-bacteria has been rarely explored. The few proof-of-concept studies are focused on: i) CO_2 sequestration and concomitant valuable product recovery by coupling algae and phototrophic bacteria in MES (Das et al., 2019), or ii) the production of bio-oil with heterotrophic microalgae using the short-chain fatty acids produced in MES as influent (Bolognesi et al., 2022).

5. Conclusions

Resilient and robust electroactive biofilms are required for efficient microbial electrosynthesis. However, more fundamental knowledge on early biofilm development and electron transfer mechanisms is required. Strategies to promote biofilm growth should focus on biocompatible 3D-structured electrodes, continuous cell operation, and favourable operation and hydrodynamic conditions to avoid mass transfer limitation and ensure availability of substrate and reducing equivalents. Diffusion of toxic molecules from the counter electrode reactions must be avoided. Promising novel approaches such as simulation and modelling tools or 3D printing of synthetic biofilms should be further investigated. In addition, long-term studies on real CO_2-containing flue gases are required to evaluate cathodic biofilms under industry relevant conditions.

Declaration of Competing Interest

The authors declare that they have no known competing financial interests or personal relationships that could have appeared to influence the work reported in this paper.

Acknowledgements

I.V. and M.K. acknowledge the funding from Academy of Finland (grant numbers 316657, 319910, 346046, and 329227). P.D. acknowledges the funding from Science Foundation Ireland (SFI) Pathfinder Award on "Hybrid Bio-Solar Reactors for wastewater treatment and CO_2 recycling" (award nr. 19/FIP/ZE/7572PF). S.P. is a Serra Hunter Fellow (UdG-AG-575) and acknowledges the funding from the ICREA Academia award and the Spanish Ministry of Science and Innovation (RTI2018-098360-B-I00 and PLEC2021-007802). LEQUIA has been recognized as a consolidated research group by the Catalan Government (2017-SGR-1552). Special thanks go to Helena Reiswich for designing the layout of Figs. 1 and 2, and the graphical abstract. We also acknowledge the COST Action CA19123 PHOENIX: Protection, resilience and rehabilitation of damaged environment.

Appendix A. Supplementary data

Supplementary data to this article can be found online at https://doi.org/10.1016/j.biortech.2022.126788.

References

Alqahtani, M.F., Katuri, K.P., Bajracharya, S., Yu, Y., Lai, Z., Saikaly, P.E., 2018. Porous hollow fiber nickel electrodes for effective supply and reduction of carbon dioxide to methane through microbial electrosynthesis. Adv. Funct. Mater. 28 (43), 1804860. https://doi.org/10.1002/adfm.v28.4310.1002/adfm.201804860.

Ameen, F., Alshehri, W.A., Nadhari, S.A., 2020. Effect of electroactive biofilm formation on acetic acid production in anaerobic sludge driven microbial electrosynthesis. ACS Sustain. Chem. Eng. 8 (1), 311–318.

Anwer, A.H., Khan, N., Khan, M.D., Shakeel, S., Khan, M.Z., 2021. Redox mediators as cathode catalyst to boost the microbial electro-synthesis of biofuel product from carbon dioxide. Fuel 302, 121124. https://doi.org/10.1016/j.fuel.2021.121124.

Arends, J., 2013. Optimizing the plant microbial fuel cell: diversifying applications and product outputs. Ph.D. thesis.

Babauta, J.T., Beyenal, H., 2014. Mass transfer studies of *Geobacter sulfurreducens* biofilms on rotating disk electrodes. Biotechnol. Bioeng. 111 (2), 285–294.

Bajracharya, S., Vanbroekhoven, K., Buisman, C.J.N., Pant, D., Strik, D.P.B.T.B., 2016. Application of gas diffusion biocathode in microbial electrosynthesis from carbon dioxide. Environ. Sci. Pollut. Res. 23 (22), 22292–22308.

Batlle-Vilanova, P., Puig, S., Gonzalez-Olmos, R., Vilajeliu-Pons, A., Balaguer, M.D., Colprim, J., 2015. Deciphering the electron transfer mechanisms for biogas

upgrading to biomethane within a mixed culture biocathode. RSC Adv. 5 (64), 52243–52251.
Berlanga, M., Guerrero, R., 2016. Living together in biofilms: the microbial cell factory and its biotechnological implications. Microb Cell Fact 15 (1). https://doi.org/10.1186/s12934-016-0569-5.
Blanchet, E., Duquenne, F., Rafrafi, Y., Etcheverry, L., Erable, B., Bergel, A., 2015. Importance of the hydrogen route in up-scaling electrosynthesis for microbial CO_2 reduction. Energy Environ. Sci. 8 (12), 3731–3744.
Blasco-Gómez, R., Ramió-Pujol, S., Bañeras, L., Colprim, J., Balaguer, M.D., Puig, S., 2019. Unravelling the factors that influence the bio-electrorecycling of carbon dioxide towards biofuels. Green Chem. 21 (3), 684–691.
Bolognesi, S., Bañeras, L., Perona-Vico, E., Capodaglio, A.G., Balaguer, M.D., Puig, S., 2021. Carbon dioxide to bio-oil in a bioelectrochemical system-assisted microalgae biorefinery process. Sustain. Energy Fuels 6 (1), 150–161.
Buckel, W., Thauer, R.K., 2018. Flavin-based electron bifurcation, a new mechanism of biological energy coupling. Chem. Rev. 118 (7), 3862–3886.
Cabau-Peinado, O., Straathof, A.J.J., Jourdin, L., 2021. A general model for biofilm-driven microbial electrosynthesis of carboxylates from CO_2. Front. Microbiol. 12 https://doi.org/10.3389/fmicb.2021.66921810.3389/fmicb.2021.669218.s00110.3389/fmicb.2021.669218.s002.
Chen, S., Rotaru, A.E., Shrestha, P.M., Malvankar, N.S., Liu, F., Fan, W., Nevin, K.P., Lovley, D.R., 2014. Promoting interspecies electron transfer with biochar. Sci. Rep. 4.
Cheng, S., Xing, D., Call, D.F., Logan, B.E., 2009. Direct biological conversion of electrical current into methane by electromethanogenesis. Environ. Sci. Technol. 43 (10), 3953–3958.
Claassens, N.J., Cotton, C.A.R., Kopljar, D., Bar-Even, A., 2019. Making quantitative sense of electromicrobial production. Nat. Catal. 2 (5), 437–447.
Costerton, J.W., Lewandowski, Z., Caldwell, D.E., Korber, D.R., Lappin-Scott, H.M., 1995. Microbial biofilms. Annual Rev. Microbiol. 49 (1), 711–745.
Das, S., Das, I., Ghangrekar, M.M., 2020. Role of applied potential on microbial electrosynthesis of organic compounds through carbon dioxide sequestration. J. Environ. Chem. Eng. 8 (4), 104028. https://doi.org/10.1016/j.jece:2020.104028.
Das, S., Das, S., Das, I., Ghangrekar, M.M., 2019. Application of bioelectrochemical systems for carbon dioxide sequestration and concomitant valuable recovery: A review. Mater. Sci. Energy Technol. 2 (3), 687–696.
Das, S., Das, S., Ghangrekar, M.M., 2021. Application of TiO_2 and Rh as cathode catalyst to boost the microbial electrosynthesis of organic compounds through CO_2 sequestration. Process Biochem. 101, 237–246.
Dessì, P., Rovira-Alsina, L., Sánchez, C., Dinesh, G.K., Tong, W., Chatterjee, P., Tedesco, M., Farràs, P., Hamelers, H.M.V., Puig, S., 2021a. Microbial electrosynthesis: towards sustainable biorefineries for production of green chemicals from CO_2 emissions. Biotechnol. Adv. 46, 107675. https://doi.org/10.1016/j.biotechadv.2020.107675.
Dessì, P., Sánchez, C., Mills, S., Cocco, F.G., Isipato, M., Ijaz, U.Z., Collins, G., Lens, P.N. L., 2021b. Carboxylic acids production and electrosynthetic microbial community evolution under different CO_2 feeding regimens. Bioelectrochemistry 137, 107686. https://doi.org/10.1016/j.bioelechem.2020.107686.
Deutzmann, J.S., Sahin, M., Spormann, A.M., Harwood, C.S., 2015. Extracellular enzymes facilitate electron uptake in biocorrosion and bioelectrosynthesis. MBio 6 (2). https://doi.org/10.1128/mBio.00496-15.
Dong, Z., Wang, H., Tian, S., Yang, Y., Yuan, H., Huang, Q., Song, T. shun, Xie, J., 2018. Fluidized granular activated carbon electrode for efficient microbial electrosynthesis of acetate from carbon dioxide. Bioresour. Technol. 269, 203–209.
Faraghiparapari, N., Zengler, K., 2017. Production of organics from CO_2 by microbial electrosynthesis (MES) at high temperature. J. Chem. Technol. Biotechnol. 92 (2), 375–381.
Flemming, H.-C., Wingender, J., 2010. The biofilm matrix. Nat. Rev. Microbiol. 89 (8), 623–633.
Flexer, V., Jourdin, L., 2020. Purposely designed hierarchical porous electrodes for high rate microbial electrosynthesis of acetate from carbon dioxide. Acc. Chem. Res. 53 (2), 311–321.
Fontmorin, J.-M., Izadi, P., Li, D.a., Lim, S.S., Farooq, S., Bilal, S.S., Cheng, S., Yu, E.H., 2021. Gas diffusion electrodes modified with binary doped polyaniline for enhanced CO_2 conversion during microbial electrosynthesis. Electrochim. Acta 372, 137853. https://doi.org/10.1016/j.electacta.2021.137853.
Gibson, B., Wilson, D.J., Feil, E., Eyre-Walker, A., 2018. The distribution of bacterial doubling times in the wild. Proc. R. Soc. B Biol. Sci. 285 (1880), 20180789. https://doi.org/10.1098/rspb.2018.0789.
Gimkiewicz, C., Hegner, R., Gutensohn, M.F., Koch, C., Harnisch, F., 2017. Study of electrochemical reduction of CO_2 for future use in secondary microbial electrochemical technologies. ChemSusChem 10 (5), 958–967.
Hackbarth, M., Jung, T., Reiner, J.E., Gescher, J., Horn, H., Hille-Reichel, A., Wagner, M., 2020. Monitoring and quantification of bioelectrochemical *Kyrpidia spormannii* biofilm development in a novel flow cell setup. Chem. Eng. J. 390, 124604. https://doi.org/10.1016/j.cej.2020.124604.
Halan, B., Buehler, K., Schmid, A., 2012. Biofilms as living catalysts in continuous chemical syntheses. Trends Biotechnol. 30 (9), 453–465.
Halan, B., Letzel, T., Schmid, A., Buehler, K., 2014. Solid support membrane-aerated catalytic biofilm reactor for the continuous synthesis of (S)-styrene oxide at gram scale. Biotechnol. J. 9 (10), 1339–1349.
Hou, X., Huang, L., 2020. Synergetic magnetic field and loaded Fe_3O_4 for simultaneous efficient acetate production and Cr(VI) removal in microbial electrosynthesis systems. Chem. Eng. J. Adv. 2, 100019. https://doi.org/10.1016/j.ceja.2020.100019.
Hou, X., Huang, L., Zhou, P., 2021. Synergetic interaction of magnetic field and loaded magnetite for enhanced acetate production in biocathode of microbial electrosynthesis system. Int. J. Hydrogen Energy 46 (10), 7183–7194.
Huang, H., Huang, Q., Song, T.-S., Xie, J., 2020. In situ growth of Mo_2C on cathodes for efficient microbial electrosynthesis of acetate from CO_2. Energy Fuels 34 (9), 11299–11306.
Huang, H., Wang, H., Huang, Q., Song, T.-S., Xie, J., 2021. Mo_2C/N-doped 3D loofah sponge cathode promotes microbial electrosynthesis from carbon dioxide. Int. J. Hydrogen Energy 46 (39), 20325–20337.
Izadi, P., Fontmorin, J.-M., Godain, A., Yu, E.H., Head, I.M., 2020. Parameters influencing the development of highly conductive and efficient biofilm during microbial electrosynthesis: the importance of applied potential and inorganic carbon source. npj Biofilms Microbiomes 6, 40.
Jiang, Y., Liang, Q., Chu, N.a., Hao, W., Zhang, L., Zhan, G., Li, D., Zeng, R.J., 2020. A slurry electrode integrated with membrane electrolysis for high-performance acetate production in microbial electrosynthesis. Sci. Total Environ. 741, 140198. https://doi.org/10.1016/j.scitotenv.2020.140198.
Jourdin, L., Grieger, T., Monetti, J., Flexer, V., Freguia, S., Lu, Y., Chen, J., Romano, M., Wallace, G.G., Keller, J., 2015. High acetic acid production rate obtained by microbial electrosynthesis from carbon dioxide. Environ. Sci. Technol. 49 (22), 13566–13574.
Jourdin, L., Raes, S.M.T., Buisman, C.J.N., Strik, D.P.B.T.B., 2018. Critical biofilm growth throughout unmodified carbon felts allows continuous bioelectrochemical chain elongation from CO_2 up to caproate at high current density. Front. Energy Res. 6, 7.
Jourdin, L., Sousa, J., Stralen, N.V., Strik, D.P.B.T.B., 2020. Techno-economic assessment of microbial electrosynthesis from CO_2 and/or organics: An interdisciplinary roadmap towards future research and application. Appl. Energy 279, 115775. https://doi.org/10.1016/j.apenergy.2020.115775.
Karthikeyan, R., Singh, R., Bose, A., 2019. Microbial electron uptake in microbial electrosynthesis: a mini-review. J. Ind. Microbiol. Biotechnol. 46 (9-10), 1419–1426.
Katsyv, A., Müller, V., 2020. Overcoming energetic barriers in acetogenic C1 conversion. Front. Bioeng. Biotechnol. 1420.
Kracke, F., Deutzmann, J.S., Jayathilake, B.S., Pang, S.H., Chandrasekaran, S., Baker, S. E., Spormann, A.M., 2021. Efficient hydrogen delivery for microbial electrosynthesis via 3D-printed cathodes. Front. Microbiol. 12 https://doi.org/10.3389/fmicb.2021.69647310.3389/fmicb.2021.696473.s00110.3389/fmicb.2021.696473.s00210.3389/fmicb.2021.696473.s003.
Kracke, F., Vassilev, I., Krömer, J.O., 2015. Microbial electron transport and energy conservation - The foundation for optimizing bioelectrochemical systems. Front. Microbiol. 6, 1–18.
Krige, A., Rova, U., Christakopoulos, P., 2021. 3D bioprinting on cathodes in microbial electrosynthesis for increased acetate production rate using Sporomusa ovata. J. Environ. Chem. Eng. 9 (5), 106189. https://doi.org/10.1016/j.jece:2021.106189.
Lai, A., Aulenta, F., Mingazzini, M., Palumbo, M.T., Papini, M.P., Verdini, R., Majone, M., 2017. Bioelectrochemical approach for reductive and oxidative dechlorination of chlorinated aliphatic hydrocarbons (CAHs). Chemosphere 169, 351–360.
Li, J., Li, Z., Xiao, S., Fu, Q., Kobayashi, H., Zhang, L., Liao, Q., Zhu, X., 2020a. Startup cathode potentials determine electron transfer behaviours of biocathodes catalysing CO_2 reduction to CH_4 in microbial electrosynthesis. J. CO_2 Util. 35, 169–175.
Li, Q., Fu, Q., Kobayashi, H., He, Y., Li, Z., Li, J., Liao, Q., Zhu, X., 2020b. GO/PEDOT modified biocathodes promoting CO_2 reduction to CH_4 in microbial electrosynthesis. Sustain. Energy Fuels 4 (6), 2987–2997.
Lovley, D.R., 2017. Syntrophy goes electric: direct interspecies electron transfer. Annu. Rev. Microbiol. 71 (1), 643–664.
Mand, T.D., Metcalf, W.W., 2019. Energy conservation and hydrogenase function in methanogenic archaea, in particular the genus *Methanosarcina*. Microbiol. Mol. Biol. Rev. 83, e00020–19.
Marshall, C.W., Ross, D.E., Handley, K.M., Weisenhorn, P.B., Edirisinghe, J.N., Henry, C. S., Gilbert, J.A., May, H.D., Norman, R.S., 2017. Metabolic Reconstruction and Modeling Microbial Electrosynthesis. Sci Rep 7 (1). https://doi.org/10.1038/s41598-017-08877-z.
Martinez, C.M., Alvarez, L.H., 2018. Application of redox mediators in bioelectrochemical systems. Biotechnol. Adv. 36 (5), 1412–1423.
Mohanakrishna, G., Abu Reesh, I.M., Vanbroekhoven, K., Pant, D., 2020. Microbial electrosynthesis feasibility evaluation at high bicarbonate concentrations with enriched homoacetogenic biocathode. Sci. Total Environ. 715, 137003. https://doi.org/10.1016/j.scitotenv.2020.137003.
Nevin, K.P., Hensley, S.A., Franks, A.E., Summers, Z.M., Ou, J., Woodard, T.L., Snoeyenbos-West, O.L., Lovley, D.R., 2011. Electrosynthesis of organic compounds from carbon dioxide is catalyzed by a diversity of acetogenic microorganisms. Appl. Environ. Microbiol. 77 (9), 2882–2886.
Nevin, K.P., Woodard, T.L., Franks, A.E., Summers, Z.M., Lovley, D.R., Colwell, R.R., 2010. Microbial electrosynthesis: feeding microbes electricity to convert carbon dioxide and water to multicarbon extracellular organic compounds. MBio 1 (2). https://doi.org/10.1128/mBio.00103-10.
Nie, H., Zhang, T., Cui, M., Lu, H., Lovley, D.R., Russell, T.P., 2013. Improved cathode for high efficient microbial-catalyzed reduction in microbial electrosynthesis cells. Phys. Chem. Chem. Phys. 15 (34), 14290. https://doi.org/10.1039/c3cp52697f.
Perona-Vico, E., Feliu-Paradeda, L., Puig, S., Bañeras, L., 2020. Bacteria coated cathodes as an in-situ hydrogen evolving platform for microbial electrosynthesis. Sci. Rep. 10, 19852.
Prévoteau, A., Carvajal-Arroyo, J.M., Ganigué, R., Rabaey, K., 2020. Microbial electrosynthesis from CO_2: forever a promise? Curr. Opin. Biotechnol. 62, 48–57.
Qian, Y., Huang, L., Zhou, P., Tian, F., Puma, G.L., 2019. Reduction of Cu(II) and simultaneous production of acetate from inorganic carbon by Serratia Marcescens

biofilms and plankton cells in microbial electrosynthesis systems. Sci. Total Environ. 666, 114–125.
Romans-Casas, M., Blasco-Gómez, R., Colprim, J., Balaguer, M.D., Puig, S., 2021. Bio-electro CO_2 recycling platform based on two separated steps. J. Environ. Chem. Eng. 9 (5), 105909. https://doi.org/10.1016/j.jece:2021.105909.
Rotaru, A.-E., Shrestha, P.M., Liu, F., Markovaite, B., Chen, S., Nevin, K.P., Lovley, D.R., Voordouw, G., 2014. Direct interspecies electron transfer between *Geobacter metallireducens* and *Methanosarcina barkeri*. Appl. Environ. Microbiol. 80 (15), 4599–4605.
Rovira-Alsina, L., Balaguer, M.D., Puig, S., 2021. Thermophilic bio-electro carbon dioxide recycling harnessing renewable energy surplus. Bioresour. Technol. 321, 124423. https://doi.org/10.1016/j.biortech.2020.124423.
Rowe, A.R., Xu, S., Gardel, E., Bose, A., Girguis, P., Amend, J.P., El-Naggar, M.Y., Ribbe, M.W., 2019. Methane-linked mechanisms of electron uptake from cathodes by methanosarcina barkeri. MBio 10 (2). https://doi.org/10.1128/mBio.02448-18.
Shi, X.-C., Tremblay, P.-L., Wan, L., Zhang, T., 2021. Improved robustness of microbial electrosynthesis by adaptation of a strict anaerobic microbial catalyst to molecular oxygen. Sci. Total Environ. 754, 142440. https://doi.org/10.1016/j.scitotenv.2020.142440.
Song, J., Kim, Y., Lim, M., Lee, H., Lee, J.I., Shin, W., 2011. Microbes as electrochemical CO_2 conversion catalysts. ChemSusChem 4 (5), 587–590.
Song, T.-S., Zhang, H., Liu, H., Zhang, D., Wang, H., Yang, Y., Yuan, H., Xie, J., 2017. High efficiency microbial electrosynthesis of acetate from carbon dioxide by a self-assembled electroactive biofilm. Bioresour. Technol. 243, 573–582.
Song, T.-S., Fu, L., Wan, N., Wu, J., Xie, J., 2020a. Hydrothermal synthesis of MoS_2 nanoflowers for an efficient microbial electrosynthesis of acetate from CO_2. J. CO2 Util. 41, 101231. https://doi.org/10.1016/j.jcou.2020.101231.
Song, X.u., Huang, L., Lu, H., Zhou, P., Wang, M., Li, N., 2020b. An external magnetic field for efficient acetate production from inorganic carbon in Serratia marcescens catalyzed cathode of microbial electrosynthesis system. Biochem. Eng. J. 155, 107467. https://doi.org/10.1016/j.bej.2019.107467.
Sousa, F.L., Martin, W.F., 2014. Biochemical fossils of the ancient transition from geoenergetics to bioenergetics in prokaryotic one carbon compound metabolism. Biochim. Biophys. Acta - Bioenerg. 1837 (7), 964–981.
Srikanth, S., Kumar, M., Singh, D., Singh, M.P., Puri, S.K., Ramakumar, S.S.V., 2018. Long-term operation of electro-biocatalytic reactor for carbon dioxide transformation into organic molecules. Bioresour. Technol. 265, 66–74.
Sun, D., Chen, J., Huang, H., Liu, W., Ye, Y., Cheng, S., 2016. The effect of biofilm thickness on electrochemical activity of *Geobacter sulfurreducens*. Int. J. Hydrogen Energy 41 (37), 16523–16528.
Sun, D., Cheng, S., Wang, A., Li, F., Logan, B.E., Cen, K., 2015. Temporal-spatial changes in viabilities and electrochemical properties of anode biofilms. Environ. Sci. Technol. 49 (8), 5227–5235.
Tahir, K., Miran, W., Jang, J., Woo, S.H., Lee, D.S., 2021. Enhanced product selectivity in the microbial electrosynthesis of butyrate using a nickel ferrite-coated biocathode. Environ. Res. 196, 110907. https://doi.org/10.1016/j.envres.2021.110907.
Thatikayala, D., Min, B., 2021. Copper ferrite supported reduced graphene oxide as cathode materials to enhance microbial electrosynthesis of volatile fatty acids from CO_2. Sci. Total Environ. 768, 144477. https://doi.org/10.1016/j.scitotenv.2020.144477.
Thauer, R.K., Kaster, A.-K., Seedorf, H., Buckel, W., Hedderich, R., 2008. Methanogenic archaea: ecologically relevant differences in energy conservation. Nat. Rev. Microbiol. 2008 68 6, 579–591.
Tian, S., He, J., Huang, H., Song, T.-S., Wu, X., Xie, J., Zhou, W., 2020a. Perovskite-based multifunctional cathode with simultaneous supplementation of substrates and electrons for enhanced microbial electrosynthesis of organics. ACS Appl. Mater. Interfaces 12 (27), 30449–30456.
Tian, S., Yao, X., Song, T.-S., Chu, Z., Xie, J., Jin, W., 2020b. Artificial electron mediator with nanocubic architecture highly promotes microbial electrosynthesis from carbon dioxide. ACS Sustain. Chem. Eng. 8 (17), 6777–6785.
Tremblay, P.-L., Angenent, L.T., Zhang, T., 2017. Extracellular electron uptake: among autotrophs and mediated by surfaces. Trends Biotechnol. 35 (4), 360–371.
Vassilev, I., Hernandez, P.A., Batlle-Vilanova, P., Freguia, S., Krömer, J.O., Keller, J., Ledezma, P., Virdis, B., 2018. Microbial electrosynthesis of isobutyric, butyric, caproic acids, and corresponding alcohols from carbon dioxide. ACS Sustain. Chem. Eng. 6 (7), 8485–8493.
Viggi, C.C., Colantoni, S., Falzetti, F., Bacaloni, A., Montecchio, D., Aulenta, F., 2020. Conductive magnetite nanoparticles enhance the microbial electrosynthesis of acetate from CO_2 while diverting electrons away from methanogenesis. Fuel Cells 20 (1), 98–106.
Wang, G., Huang, Q., Song, T.-S., Xie, J., 2020. Enhancing microbial electrosynthesis of acetate and butyrate from CO_2 reduction involving engineered *Clostridium ljungdahlii* with a nickel-phosphide-modified electrode. Energy Fuels 34 (7), 8666–8675.
Wood, J.C., Grové, J., Marcellin, E., Heffernan, J.K., Hu, S., Yuan, Z., Virdis, B., 2021. Strategies to improve viability of a circular carbon bioeconomy-A techno-economic review of microbial electrosynthesis and gas fermentation. Water Res. 201, 117306. https://doi.org/10.1016/j.watres.2021.117306.
Xiang, Y., Liu, G., Zhang, R., Lu, Y., Luo, H., 2017. Acetate production and electron utilization facilitated by sulfate-reducing bacteria in a microbial electrosynthesis system. Bioresour. Technol. 241, 821–829.
Xiao, S., Fu, Q., Xiong, K., Li, Z., Li, J., Zhang, L., Liao, Q., Zhu, X., 2020. Parametric study of biocathodes in microbial electrosynthesis for CO_2 reduction to CH_4 with a direct electron transfer pathway. Renew. Energy 162, 438–446.
Xu, B., Li, Z., Jiang, Y., Chen, M., Chen, B., Xin, F., Dong, W., Jiang, M., 2022. Recent advances in the improvement of bi-directional electron transfer between abiotic/biotic interfaces in electron-assisted biosynthesis system. Biotechnol. Adv. 54, 107810. https://doi.org/10.1016/j.biotechadv.2021.107810.
Yang, H.-Y., Hou, N.-N., Wang, Y.-X., Liu, J., He, C.-S., Wang, Y.-R., Li, W.-H., Mu, Y., 2021. Mixed-culture biocathodes for acetate production from CO_2 reduction in the microbial electrosynthesis: Impact of temperature. Sci. Total Environ. 790, 148128. https://doi.org/10.1016/j.scitotenv.2021.148128.
Yang, H.-Y., Wang, Y.-X., He, C.-S., Qin, Y., Li, W.-Q., Li, W.-H., Mu, Y., 2020. Redox mediator-modified biocathode enables highly efficient microbial electro-synthesis of methane from carbon dioxide. Appl. Energy 274, 115292. https://doi.org/10.1016/j.apenergy.2020.115292.
Yee, M.O., Rotaru, A.-E., 2020. Extracellular electron uptake in *Methanosarcinales* is independent of multiheme c-type cytochromes. Sci. Reports 2020 (10), 372.
Yong, X., Enhua, Z., Jingdong, Z., Youfen, D., Zhaohui, Y., M., C.H.E., Jens, U., Feng, Z., 2022. Extracellular polymeric substances are transient media for microbial extracellular electron transfer. Sci. Adv. 3, e1700623.
Yu, L., Yuan, Y., Tang, J., Zhou, S., 2017. Thermophilic *Moorella thermoautotrophica*-immobilized cathode enhanced microbial electrosynthesis of acetate and formate from CO_2. Bioelectrochemistry 117, 23–28.
Zhou, H., Xing, D., Xu, M., Su, Y., Ma, J., Angelidaki, I., Zhang, Y., 2021. Optimization of a newly developed electromethanogenesis for the highest record of methane production. J. Hazard. Mater. 407, 124363. https://doi.org/10.1016/j.jhazmat.2020.124363.